



THE UNIVERSITY *of* EDINBURGH

Edinburgh Research Explorer

Tissue-specific host recognition by complement factor H is mediated by differential activities of its glycosaminoglycan-binding regions

Citation for published version:

Clark, SJ, Ridge, LA, Herbert, AP, Hakobyan, S, Mulloy, B, Lennon, R, Würzner, R, Morgan, BP, Uhrin, D, Bishop, PN & Day, AJ 2013, 'Tissue-specific host recognition by complement factor H is mediated by differential activities of its glycosaminoglycan-binding regions' *Journal of Immunology*, vol. 190, no. 5, pp. 2049-57. DOI: 10.4049/jimmunol.1201751

Digital Object Identifier (DOI):

[10.4049/jimmunol.1201751](https://doi.org/10.4049/jimmunol.1201751)

Link:

[Link to publication record in Edinburgh Research Explorer](#)

Document Version:

Peer reviewed version

Published In:

Journal of Immunology

Publisher Rights Statement:

Copyright © 2013 by The American Association of Immunologists, Inc. All rights reserved.

General rights

Copyright for the publications made accessible via the Edinburgh Research Explorer is retained by the author(s) and / or other copyright owners and it is a condition of accessing these publications that users recognise and abide by the legal requirements associated with these rights.

Take down policy

The University of Edinburgh has made every reasonable effort to ensure that Edinburgh Research Explorer content complies with UK legislation. If you believe that the public display of this file breaches copyright please contact openaccess@ed.ac.uk providing details, and we will remove access to the work immediately and investigate your claim.



Published in final edited form as:

J Immunol. 2013 March 1; 190(5): 2049–2057. doi:10.4049/jimmunol.1201751.

Tissue-specific host recognition by complement factor H is mediated by differential activities of its glycosaminoglycan-binding regions

Simon J. Clark^{*,†}, Liam A. Ridge^{*}, Andrew P. Herbert[‡], Svetlana Hakobyan[§], Barbara Mulloy[¶], Rachel Lennon^{*}, Reinhard Würzner^{||}, B. Paul Morgan[§], Dusan Uhrin[‡], Paul N. Bishop^{†,1}, and Anthony J. Day^{*,1}

^{*}Wellcome Trust Centre for Cell-Matrix Research, Faculty of Life Sciences, University of Manchester, Oxford Road, Manchester, M13 9PT, UK

[†]Centre for Ophthalmology & Vision Research, Institute of Human Development, University of Manchester and Centre for Advanced Discovery & Experimental Therapeutics, Central Manchester University Hospitals NHS Foundation Trust, Manchester Academic Health Science Centre

[‡]Edinburgh Biomolecular NMR Unit, EaSTCHEM School of Chemistry, University of Edinburgh, West Mains Road, Edinburgh, EH9 3JJ, UK

[§]Complement Biology Group, Institute of Infection and Immunity, School of Medicine, Cardiff University, Cardiff, CF14 4XN, UK

[¶]National Institute of Biological Standards and Control, Blanche Lane, South Mimms, Potter's Bar, EN6 3QG, UK

^{||}Division of Hygiene and Med. Microbiology, Innsbruck Medical University, Innsbruck, Austria

Abstract

Complement factor H (CFH) regulates complement activation in host tissues through its recognition of polyanions, which mediate CFH binding to host cell surfaces and extracellular matrix, promoting the deactivation of deposited C3b. These polyanions include heparan sulfate (HS), a glycosaminoglycan (GAG) with a highly diverse range of structures, for which two regions of CFH (referred to as CCP6-8 and CCP19-20) have been implicated in HS binding. Mutations/polymorphisms within these GAG-binding sites have been associated with age-related macular degeneration (AMD) and atypical hemolytic uremic syndrome (aHUS). Here we demonstrate that CFH has tissue-specific binding properties, mediated through its two HS-binding regions. Our data shows that the CCP6-8 region of CFH binds more strongly to heparin (a highly sulfated form of HS) than CCPs19-20 and that their sulfate specificities are different. Furthermore, the HS-binding site in CCPs6-8, which is affected by the AMD-associated Y402H polymorphism, plays the principle role in host tissue recognition in the human eye, whilst the CCP19-20 region makes the major contribution to the binding of CFH in the human kidney. This helps provide a biochemical explanation for the genetic basis of tissue-specific diseases such as AMD and aHUS, and leads to a better understanding of the pathogenic mechanisms for these diseases of complement dysregulation.

¹To whom correspondence should be addressed: Prof. Anthony J Day Faculty of Life Sciences Manchester Michael Smith Building Oxford Road Manchester M13 9PT anthony.day@manchester.ac.uk Tel: +44 (0)161 27 51495 or Prof. Paul N. Bishop Institute of Human Development University AV Hill Building Road 9PT paul.n.bishop@manchester.ac.uk Tel: +44 (0)161 275 5755 .

Introduction

Complement factor H (CFH), a 155-kDa plasma protein, is the main regulator of the alternative pathway of complement, a key component of the innate immune response. The presence of CFH in tissues (where it is bound to host surfaces) leads to the breakdown of any deposited C3b that would otherwise result in complement amplification (1). While other proteins exert regulatory activity on host cell surfaces, i.e. CD35, CD46 and CD55 (2), CFH is the only alternative pathway regulator to confer protection to extracellular matrix (ECM) structures such as basement membranes (3,4). Impaired CFH function is a major contributing factor in the kidney disease atypical hemolytic uremic syndrome (aHUS) (5,6) and age-related macular degeneration (AMD) (7-13), which is the leading cause of blindness in the western world (14). In AMD, complement dysregulation is associated with drusen formation between the retinal pigment epithelium (RPE) and a multi-laminar ECM called Bruch's membrane (11), resulting in the destruction of the macula and consequent loss of central vision.

CFH recognizes host surfaces through its interactions with certain polyanions, such as the glycosaminoglycan (GAG) chains of proteoglycans that are present on all cells and in the ECM of host tissues (12,15,16); GAGs are long, un-branched, polysaccharides composed of disaccharide repeats that show a huge diversity in sequence based largely on variable sulfation patterns (see Supplemental Fig. 1). CFH is comprised of twenty complement control protein (CCP) domains (17) (also referred to as short consensus repeats or SCRs), containing two GAG-binding regions corresponding to CCPs6-8 and CCPs19-20 (18-25). Importantly, mutations and polymorphisms in these GAG-binding regions of CFH have been associated with both AMD (7-13) and aHUS (5,6), where in some cases they have been shown to affect the interaction of CFH with GAGs (12,20,23,25). For example, the Y402H polymorphism of CFH (26), a major risk factor for AMD (7-10,27), alters its binding to the GAGs heparin, heparan sulfate (HS) and dermatan sulfate (DS) (12,20,23) through a tyrosine to histidine substitution at residue 402 within CCP7.

Functional changes within the CFH protein, caused by mutations/polymorphisms, could alter its ability to bind host surfaces. The current understanding is that CCPs19-20 are chiefly responsible for host-recognition (28), which is consistent with the large number of polymorphisms/mutations in this region associated with aHUS (5,6). However, with the exception of R1210C (13), mutations/polymorphisms in CCPs19-20 are not associated with an increased risk of developing AMD, and the Y402H polymorphism has no effect on the susceptibility of an individual to develop aHUS. We found previously that the Y402H polymorphism had a significant effect on the binding specificity of CFH for sulfated GAGs (20,23) and that the 402H form of CFH bound less well to the Bruch's membrane of human macula, where this interaction was mediated, at least in part, by the GAGs HS and DS (12). Poorer binding of the AMD-associated 402H variant to this ECM could lead to reduced complement regulation at this site resulting in chronic local inflammation and thereby promoting the tissue damage and drusen formation that characterize AMD (3,4,12). On this basis we have hypothesized that the two GAG-binding sites have tissue-specific activities, potentially via their recognition of different HS structures. In order to test this hypothesis we have compared the GAG-binding specificities of CCP6-8 and CCP19-20 and have investigated their relative contributions to the interactions of CFH with human eye and kidney tissues.

Materials and Methods

Expression of complement factor H reagents

The 402H and 402Y polymorphic variants of fICFH were purified from the plasma of genotyped donors who were homozygous for either allele, as described in (29); these preparations each had isoleucine at position 62. Recombinant proteins representing the 402H and 402Y variants of CFH and comprising CCPs6-8 were expressed in *E. coli*, refolded and purified as described previously (20). A recombinant protein comprising CCPs19-20 of CFH (designated as residues 1107 to 1231 in the published CFH sequence, UniProt no. P08603) was expressed in *P. pastoris* as described previously (21); this recombinant protein sequence also includes the non-authentic tetrapeptide EAEF at the N-terminus. All of the recombinant proteins (which come from non-glycosylated regions of CFH (17)) have been shown previously to be correctly folded (20,21,23).

Fluorescent labeling and biotinylation of proteins and GAG reagents

The fluorescent labeling of the 402H and 402Y variants of CFH (both CCP6-8 and full-length proteins) with AlexaFluor594 and AlexaFluor488, respectively, was done as described previously (12). Labeling of the CCP19-20 recombinant protein with AlexaFluor488 was carried out in an identical manner, using the same protein labeling kit (Molecular Probes, Paisley, UK) in the presence of 10-fold molar excess of heparin dp24 oligosaccharide (Iduron, Manchester, UK) in order to protect the GAG-binding site. The heparin dp24 was removed from the labeled CCP19-20 protein by exhaustive dialysis against PBS supplemented with 1 M NaCl using 10-kDa molecular weight cut-off snakeskin dialysis tubing (Pierce, Cramlington, UK) in the dark at 4°C, as described previously (12). The labeling efficiency was calculated to be 1.5 moles fluorophore per mole of protein (the same degree of labeling as for the CCP6-8 proteins (12)). Labeling of the CCP19-20 protein was shown to have no major effect on its heparin binding properties by affinity chromatography (data not shown). Biotinylation of the CCP6-8 and CCP19-20 recombinant proteins, also performed in the presence of 10-fold molar excess heparin dp24 oligosaccharide (Iduron) to protect the GAG-binding region, was carried out using the same methodology as employed previously (20).

Biotinylation of the 2nd international standard (2IS) of heparin (30), C4S, C6S and DS were carried out as described in Clark *et al.* 2006 (20). Biotinylation of hyaluronan (HA) was carried out essentially as described previously (31). Briefly, medical grade HA (Lifecore Biomedical, Chaska, USA) was dissolved overnight in 0.1 M MES, pH5.5 at a concentration of 5 mg/ml. To 1 ml of this solution 13 µl of 25 mg/ml 1-ethyl-3-(3-dimethylaminopropyl)carbo-dimide hydrochloride (EDAC; Sigma, Poole, UK) in 0.1 M MES, pH 6.5, and 20 µl of 50mM Biotin-LC-hydrazide (Pierce) in DMSO, were added simultaneously and mixed at room temperature for 16 hours. The sample was then centrifuged at ~12,000 g for 1 min to remove particulate material and the reaction mixture was dialyzed into H₂O at 4 °C for 6 hours using 10,000 Da molecular weight cut-off snakeskin dialysis tubing (Pierce).

Microtiter plate assays

The heparin-binding characteristics of the biotinylated CCP6-8 (402H and 402Y variants) and CCP19-20 recombinant proteins was analyzed using microtiter plate based assays, where 2IS (2nd International Standard) heparin (20), or one of its selectively desulfated derivatives (32,33), were immobilized non-covalently on allylamine-coated BD Heparin Binding plates (BD Biosciences, Oxford, UK) as we have described previously (20,34). The selectively desulfated samples of the 2IS heparin used in this study were: 2-O desulfated (2-O-deS); 6-O desulfated (6-O-deS); 2- and 6-O desulfated (2,6-O-deS); N-desulfated (N-deS)

and N-desulfated re-N-acetylated (N-deS/re-N-Ac). The GAGs were immobilized at 1 µg/well on BD Heparin Binding plates in a total volume of 200 µl/well PBS, overnight at room temperature. Plates were blocked for 90 minutes at 37 °C with 300 µl/well 1% (w/v) BSA in standard assay buffer (20 mM HEPES, 130 mM NaCl, 0.05% (v/v) Tween-20, pH 7.3). This standard assay buffer was used for all subsequent incubations, dilutions and washes at room temperature. Biotinylated recombinant protein was incubated with the immobilized GAGs for 4 hours at room temperature. After the plates were washed bound protein was detected by the addition of 200 µl/well of a 1:10,000 dilution of ExtrAvidin alkaline phosphatase (Sigma-Aldrich, Poole, UK) for 30 minutes at room temperature. After further washing, plates were developed using 200 µl/well of a 1 mg/ml disodium *p*-nitrophenylphosphate solution (Sigma-Aldrich) in 0.05 M Tris-HCl, 0.1 M NaCl, pH 9.3. The absorbance values at 405 nm were determined after 40 minutes of development at room temperature and corrected against blank wells (i.e., those that contained no immobilised GAGs).

Alternatively, unlabelled CCP6-8 (either the 402H or 402Y variant) or CCP19-20 recombinant proteins were adsorbed onto the wells of microtitre plates (Nunc Maxisorb, Kastrup, Denmark) at 1 µg/ml in 200 µl PBS for 16 hours at 4 °C. The ligand-binding characteristics of these immobilized proteins were determined using the biotinylated GAGs 2IS heparin, hyaluronan, C4S, C6S and DS. Plate assays were carried out in 20 mM HEPES, 130 mM NaCl, 0.05 % (v/v) Tween-20, pH 7.3 and the level of bound GAG determined as described above for the biotinylated proteins. In all these plate assays, data points were determined in duplicate and are reported as a n=4 from two independent experiments.

Fluorescent staining of human eye and kidney tissue with fICFH

Details of the human eye and kidney tissues (without AMD or kidney disease, respectively) used in this study are provided in Table 1. The staining of human tissue sections with fluorescently labeled proteins was carried out as described previously (12). Briefly, tissue sections were incubated with chilled (−20°C) histological grade acetone (Sigma-Aldrich) for twenty seconds before being thoroughly washed with PBS: every step of the protocol was preceded by a wash step, each time in PBS alone. These were then blocked with 1 mg/ml BSA, 1% (v/v) goat serum, 0.1% (v/v) Triton X-100 in PBS for 1 h at room temperature. Tissue sections were incubated with the fluorescently labelled variants of fICFH, CCP6-8 or recombinant CCP19-20 (20 µg/ml of each in 100 µl blocking buffer) for 16 h at 4°C: 'blank' (i.e. non-stained) tissue sections were incubated with blocking buffer alone. Cell nuclei were visualized using DAPI (0.3 µM final concentration) for 5 min at room temperature. Microscope cover slips were mounted using VectaShield (VectorLabs, Peterborough, UK). Endogenous expression of CFH was visualized using the anti-CFH monoclonal antibody OX23 (35) at 10 µg/ml in blocking buffer. OX23 was incubated with tissue sections for 16 h at 4°C, washed with PBS and detected using AlexaFluor 488-conjugated goat anti-mouse IgG (Molecular Probes) at a 1:5000 dilution in PBS for 2 h at room temperature.

In competition experiments, the labeled variants of fICFH (either 402H or 402Y) were added to tissue sections in the presence of either a 1-fold or 10-fold molar excess of unlabeled CCP6-8 (i.e. the respective 402H and 402Y variant) and/or CCP19-20. In other experiments, kidney tissue was pre-treated with specific HS/DS-degrading enzymes (i.e. a mixture of heparinase I, II and III and chondroitin B lyase, all from *Flavobacterium heparinum* (36,37)) before the application of either fluorescently labeled fICFH variant proteins or the anti-CFH antibody OX23; 20 units/ml of each enzyme (Sigma-Aldrich) was incubated with the tissue sections for 2 hours at 37°C followed by thorough washing with PBS before blocking.

Fluorescent microscopy and data analysis

Images of fluorescently stained human tissue were collected on a snapshot widefield microscope (Olympus BX51) using a 20x/0.30 Plan FlN objective. Microscopy images were captured using a CoolSNAP ES camera (Photo-metrics) *via* MetaVue Software (Molecular Devices). In order to prevent bleed-through of color from one channel to the next, specific band pass filter sets were used for DAPI, FITC and Texas Red. All images were processed and analyzed using ImageJ64 (version 1.40g; rsb.info.nih.gov/ij). Relative fluorescent intensities (i.e. of RPE and Bruch's membrane in the eye samples and glomeruli in the kidney samples) were determined as described previously (12). In the case of human kidney tissues, the freehand tool (in ImageJ64) was used to select ten individual glomeruli (designated in this study as the tissue within the Bowman's space) from each donor; the ten, mean fluorescence intensity values were then averaged per donor in order to compensate for varying blood vessel number per glomeruli. For both eye and kidney tissues, the gray scale images for the red and green channels were overlaid so that an identical region was compared for both wavelengths. Tissue sections from five donor eyes and three donor kidneys were analyzed to obtain mean values (\pm s.e.m.) and the statistical significance of protein binding determined using Student's t test (in KaleidaGraph v4.0), where $P < 0.05$ was considered to be significant.

Heparin affinity chromatography.

The heparin-binding properties of the CCP19-20 region of CFH was compared to the 402H and 402Y variants of both fICFH and the CCP6-8 region of CFH by affinity chromatography on a 1 ml HiTrap Heparin column (GE Healthcare, Buckinghamshire, UK) at room temperature. The column was equilibrated in 5 ml PBS (OXOID). Protein (100 μ g recombinant CCP6-8/CCP19-20 proteins or 200 μ g fICFH) was loaded onto the column in a total volume of 5 ml PBS. The column was then washed with 4 column volumes of PBS before bound protein was eluted with a linear salt gradient (over 20 m) of 0-100% buffer A (1 M NaCl in PBS) in PBS at a flow rate of 1 ml/min; fractions (1 ml) were collected throughout the protocol.

Results

CCP6-8 and CCP19-20 regions of CFH have different GAG-binding characteristics

We examined the binding of the CCP6-8 and CCP19-20 regions of CFH to the GAG heparin, a highly sulfated form of HS often used as a model for the HS found ubiquitously in human tissues; both GAGs exhibit a diverse range of sequences (see Supplemental Fig 1) (3,38). Affinity chromatography using a HiTrap heparin column revealed that recombinant CCP19-20 protein eluted at a lower salt strength when compared to the 402H and 402Y variants, either in the context of a CCP6-8 construct or full-length CFH protein (fICFH) purified from homozygous individuals (Fig. 1). Thus the CCP19-20 region has the weakest (salt-dependent) binding to heparin. However, it was apparent that fICFH demonstrated better binding to heparin than either CCP6-8 or CCP19-20. This indicates that both of these regions contribute to the strong binding of fICFH to heparin, which is consistent with a recent study (39). Consistent with the above, the CCP19-20 construct demonstrated poorer binding to heparin compared to CCP6-8 in microtiter plate assays, where these experiments were conducted in physiological buffer conditions (Supplemental Fig. 2A). Similar analyses with other GAGs indicated that CCP19-20 does not interact significantly with chondroitin-4-sulfate (C4S), chondroitin-6-sulfate (C6S), DS or hyaluronan (HA) (Supplemental Fig. 2B-E); of these GAGs only DS has been found previously to interact with CCP6-8 (12,20) and very weak binding has been reported for CCP19-20 with C6S (25).

Given the diversity of heparin/HS sequences (e.g. their wide range of sulfation patterns) we investigated the specificity of CCP19-20 (Fig. 2) in order to compare this with those of the 402H and 402Y CCP6-8 variants, which we have analyzed previously (20,23); as before, this utilized selectively desulfated derivatives of heparin (32,33) as models of HS. All the partially desulfated preparations of heparin demonstrated poorer binding to CCP19-20 than to the unmodified GAG (Fig. 2) demonstrating that the sulfate groups play a key role in this interaction. From these data it might be anticipated that highly sulfated forms of HS would be required for optimal binding to the CCP19-20 region of CFH. Thus, the sulfate specificity of the CCP19-20 region is similar to the 402H variant, in that this form of CCP6-8 was more sensitive to removal of sulfate groups compared to 402Y (20,23); the control data for the CCP6-8 402H and 402Y proteins has been included here for completeness and ease of comparison (Supplemental Fig. 3), where these were essentially the same as those obtained previously (20,23).

However, the specificities of CCP19-20 (Fig. 2) and CCP6-8 402H (Supplemental Fig. 3B) although similar are not identical; e.g. N-desulfation/re-N-acetylation of heparin has a smaller effect on CCP19-20 binding compared to the 402H variant while the converse is seen for removal of 6-O-sulfates. On this basis CCPs19-20 would be expected to recognize different HS sequences compared to CCPs6-8, which may affect the way CFH recognizes HS in human tissues.

CCPs6-8 contribute more than CCPs19-20 to CFH binding to sites in human macula

Having demonstrated that the heparin-binding strengths/specificities of the CCP6-8 and CCP19-20 regions differed from one another in experiments using purified GAG preparations, we investigated their relative contributions to binding-site recognition in human tissues. Unlabeled CCP6-8 and CCP19-20 proteins were used as competitive inhibitors for the interaction of fluorescently labeled fICFH (i.e. 402H or 402Y) with human macula tissues from non-AMD donors (age range 58-81 years; Table 1), using a modification of the method described previously (12). CCPs19-20 caused little or no inhibition of fICFH binding to the RPE or Bruch's membrane even at 10-fold molar excess (Fig. 3A); statistically significant effects were only seen for competition of the 402Y variant corresponding to ~11% and ~20% reduction in binding to the RPE and Bruch's membrane, respectively. However, when an equivalent experiment was performed with CCP6-8 a large and statistically significant decrease in binding of fICFH was observed on both RPE and Bruch's membrane (Fig. 3B); e.g. with 10-fold molar excess of CCP6-8 there was 77% inhibition of fICFH binding to the Bruch's membrane for the 402H variant. These data clearly demonstrate that CCPs6-8 make a larger contribution to binding of CFH than CCPs19-20. When the CCP6-8 and CCP19-20 proteins were used together as competitors this led to a greater level of inhibition (Fig. 3C) than that seen for CCP6-8 alone (Fig. 3B). The enhanced competition could be explained by CCPs6-8 and CCPs19-20 recognizing distinct HS structures within human macula. Overall, these results demonstrate that CCPs6-8 play a more prominent role in the interaction of CFH with human macula, although CCPs19-20 likely makes some contribution to binding in the context of the full-length CFH.

Tissue binding experiments revealed that fluorescently labeled CCP19-20 was able to bind directly to the Bruch's membrane (albeit weakly) and to the RPE (Fig. 4). The pattern of binding for CCP19-20 was similar to that for the 402H variant of CCP6-8, both of which bound less well to the Bruch's membrane compared to the 402Y form of CCP6-8; all three constructs exhibited essentially identical levels of binding to the RPE (Fig. 4C-D). This may be because CCP19-20 and CCP6-8 402H require highly sulfated HS structures for optimal binding (based on the specificities described in Fig. 2 and Supplemental Fig. 3B), of which there may be relatively few in Bruch's membrane; the broader specificity of 402Y ((20,23); and Supplemental Fig. 3A) would allow it to interact with a wide range of HS sequences

within this specialized ECM. Enzyme pretreatment of human eye sections to remove HS caused a small but significant reduction (~20%) in binding of CCP19-20 to the RPE, that was not further reduced by the additional removal of DS (Fig. 5). In the case of the Bruch's membrane there was a 55% reduction in the binding of CCP19-20 when HS alone or DS/HS together were removed. This demonstrates that the CCP19-20 region of CFH recognizes HS (but not DS) in human macula (consistent with the GAG specificity described above). However, the effect of enzyme digestion was much less marked on CCP19-20 binding compared to CCP6-8, where removal of DS/HS reduced binding by 90% (12), indicating that CCPs19-20 also recognize non-GAG ligands; staining with an anti-C3b antibody showed that there was little or no C3b in either the macula or kidney donor tissues used within this study (see Supplemental Fig. 4), indicating that C3b is unlikely to be responsible for the GAG-independent binding seen here for CFH. The results described above demonstrate that CCP6-8 has a greater role than CCP19-20 in mediating the interaction of CFH with sites in human macula, which is in agreement with previous data showing that fICFH and CCP6-8 have similar patterns of binding on Bruch's membrane, RPE and choroidal blood vessels (12).

Binding of CFH to human kidney glomeruli is mediated by the CCP19-20 region

Given the different HS-binding specificities of the CCP6-8 and CCP19-20 regions (see above), and that different tissues have HS with distinct compositions and sulfation patterns (3,38,40), we investigated whether the relative contributions of these GAG-binding regions was the same in human kidney; this tissue was chosen because of the association of mutations/polymorphisms in CCPs19-20 with aHUS (5,6). Staining with an anti-CFH antibody showed that the endogenous CFH protein is present throughout the glomerulus, being particularly prominent on the Bowman's capsule and glomerular basement membrane (GBM) (Fig. 6A). A similar staining pattern was apparent when fluorescently labeled CCP19-20 was used as a probe to detect its binding sites (Fig. 6B), whereas, neither the 402H nor 402Y variants of CCP6-8 bound significantly to this tissue (Fig. 6C). This observation suggests that the CCP19-20 region plays a more prominent role in the binding of CFH to human glomeruli compared to CCP6-8. When kidney tissue was stained with fluorescently labeled fICFH proteins both the 402H and 402Y variants bound to similar degrees throughout most of the glomerulus but with somewhat greater binding to the GBM (orange/yellow staining in Fig. 6D); the exception to this was the Bowman's capsule, where there was a higher level of 402Y fICFH (green) staining. Pre-treatment of the kidney tissue with GAG-degrading enzymes lead to a ~30-40% reduction in the fluorescence intensity observed in the glomeruli with the labeled 402H and 402Y fICFH variants (Fig. 7A) and an ~60% reduction in CCP19-20 binding (Fig. 7B). These data indicate a likely role for HS in the binding of CFH to the glomeruli of human kidneys. However, the relatively small effect of GAG removal on CCP19-20 binding in the kidney (compared to >90% reduction of CCP6-8 binding in the macula (12)) provides evidence that CCP19-20 also interacts with non-GAG ligands in this tissue.

To further assess the relative contributions of CCPs6-8 and CCPs19-20 on CFH binding to human kidney we performed competition experiments, essentially as described above for eye tissue. The CCP6-8 variant proteins caused no statistically significant inhibition of fICFH binding (Fig. 8B), whereas, the CCP19-20 protein caused ~60% inhibition when present at 10-fold molar excess (Fig. 8A). Competition of fICFH binding, using CCP6-8 and CCP19-20 together, had no greater effect than CCP19-20 alone (Fig. 8C). Overall, these data demonstrate that, in contrast to human macula, CCPs19-20 play the dominant role in the binding of CFH to sites within human kidney glomeruli, and that, at least in part, this is via its interaction with HS.

Discussion

Here, we demonstrate that the two GAG-binding regions of CFH both play a major role in the localization of the protein on host surfaces, but that the relative contribution of these regions is tissue-specific; CCPs6-8 predominate in CFH binding to the human RPE and Bruch's membrane, whereas CCPs19-20 mediate the interaction with human kidney glomeruli. These data correlate well with the evidence that the Y402H polymorphism (in CCP7) is associated with AMD (7-10,27), while mutations/polymorphisms in CCPs19-20 are associated with kidney diseases such as aHUS (5,6). Interestingly, we have also found that the mechanism underlying the tissue binding of the CCP6-8 and CCP19-20 regions differ, in that the former is mediated primarily via its interaction with sulfated GAGs, whereas a significant component of the latter is GAG-independent. Hence, while digestion of HS/DS reduces the binding of CCP6-8 by 90% in Bruch's membrane (12), removal of these GAGs leads to only a ~50% reduction in the binding of CCP19-20 to both Bruch's membrane and kidney tissue. However, from our analyses it is clear that ~50% of CCP19-20 binding, to sites in these tissues, is mediated through its interaction with HS. In this regard, while the GAG-binding specificity of CCP19-20 was shown to differ from that of CCP6-8 in the details of their sulfation requirements, it was more similar to the 402H variant (compared to 402Y) in that it bound best to highly sulfated forms of heparin. Overall these data suggest that the Bruch's membrane contains only a relatively small number of appropriately sulfated HS sequences that are able to support the binding of CCP19-20 and the 402H form of CCP6-8. Furthermore, the results of our competition experiments indicate that CCPs6-8 and CCPs19-20 recognize different HS structures in the human eye, allowing high avidity interaction of the full-length CFH protein by the utilization of two independent binding sites (i.e. even in the context of the 402H isoform of CFH).

Both AMD and aHUS are conditions thought to result from complement dysregulation brought about, at least in part, by abnormalities in CFH binding/function (6,11,12,41). The results we described here provide evidence that polymorphisms/mutations in different regions of CFH differentially affect its activity in different tissues and thus predispose to different diseases. Consistent with this, the common Y402H polymorphism is associated with AMD and not aHUS, whereas the majority of amino acid substitutions in CCPs19-20 associated with aHUS have not been linked to AMD (5,6). One exception to this is the highly penetrant, but rare, R1210C mutation in the C-terminal region of CCP20 that confers high risk of developing AMD (13). While the effects of this mutation on GAG binding have not been tested in the context of the full-length protein, it does affect the binding of CCPs8-20 to heparin (42,43), and also has a major effect on the interaction of CFH with surface bound C3b (44). Importantly, the R1210C mutant of CFH has also been shown to form a high molecular weight covalent complex with human serum albumin (44), which would have a dramatic effect on the movement of CFH through the Bruch's membrane (45) as well as masking/altering other functions (44). Thus, the association of R1210C with AMD may be independent of any effect on GAG binding. It should be noted that 60% of individuals who carry the R1210C CFH allele and have AMD also have a 402H CFH allele (13). Based on our description of the importance of CCPs6-8 in the interaction of CFH with sites in normal macula and the effect of the Y402H polymorphism on GAG binding (12,20), the impaired R1210C function would not be compensated well by the CFH 402H produced from the other allele in these patients.

Another recent study has shown that a major CFH ligand is malondialdehyde (MDA), a common lipid peroxidation product found to accumulate in diseases such as AMD as a result of oxidative stress (46); e.g. MDA is found on the surface of apoptotic/necrotic cells and blebs derived from these. Importantly, it was demonstrated that CFH binds to MDA *via* both CCPs 7 and 20, and that the Y402H polymorphism dramatically reduced binding.

Furthermore, it has been proposed that MDA-mediated CFH recruitment inhibits complement activation in regions with drusen build-up and that reduced binding of the 402H CFH variant would be pro-inflammatory (46). Thus, whilst the impaired binding of 402H to Bruch's membrane could result in local complement dysregulation contributing to disease initiation, as we have suggested previously (4,12), it could also be the case that the altered binding to ligands such as CRP (47-49), necrotic cells (46,47) and oxidized lipids (46), could be important in driving AMD progression once drusen have started to form. Both the work described here and that from Weisman and colleagues (46) provides strong evidence that the Y402H polymorphism within the CCP6-8 region of CFH plays a major role in AMD pathogenesis because of the direct effect that this has on its binding functions.

A major finding of our study is that the CCP6-8 and CCP19-20 regions of CFH differentially mediate binding in different host tissues, which occurs, at least in part, through their recognition of distinct GAG populations. It is well established that GAG composition/sequence is dependent on tissue location (3,38) and, for example, even within the different layers of the macula there is evidence for considerable diversity of GAG structure (40). In this regard, the 402H and 402Y variants (in the context of CCPs6-8) recognize different GAG sequences in human Bruch's membrane (12) and the current study demonstrates that the specificity of CCPs19-20 for HS in this ECM is different again. As noted above, the profound effect of the Y402H polymorphism on GAG binding could explain the functional basis of this polymorphism in AMD. On the other hand, the interaction of CCPs19-20 with HS clearly mediates a significant proportion of CFH binding to kidney GBM. Consistent with this, expression of glomerular heparinase has been shown to increase in patients suffering from dense deposit disease (another kidney condition associated with CFH polymorphisms/mutations in CCP19-20), where the staining of HS in the GBM decreases accordingly (50).

Given the importance of correct surface recognition by CFH on complement regulation, it is not surprising that disruption of this event can result in diseases such as AMD and aHUS. The current widely held view that one main surface-recognition region exists in CFH, and that this resides in the CCP19-20 portion of the protein, may be simplistic and, in the case of certain tissues such as the human macula, incorrect. Knowledge that the contribution to host surveillance conferred by the two GAG-binding regions of CFH alters depending on the tissue context should permit organ-specific therapeutic strategies to re-address the balance of immune regulation in AMD and other diseases of complement dysregulation.

Supplementary Material

Refer to Web version on PubMed Central for supplementary material.

Acknowledgments

Our thanks go to Dr. Isaac Zambrano at the Manchester Royal Eye Hospital Eye Bank for access to human eye tissues, and Dr. Günter Klima and Dr. Walter Rabl (Innsbruck Medical University) for providing human kidney material. We also thank Ms. Viranga Tilakaratna (University of Manchester) for preparing the biotinylated HA, Dr. Sheona Drummond (University of Manchester) for helpful discussions regarding fluorescent microscopy and Dr. Robert Sim (University of Oxford) for providing the OX23 anti-CFH antibody.

We acknowledge financial support from the Medical Research Council [Grant No. G0900592] and the Manchester NIHR Biomedical Research Centre. The Bioimaging Facility microscopes used in this study were purchased with grants from BBSRC, Wellcome Trust and the University of Manchester Strategic Fund. SJC is the grateful recipient of a Stepping Stones Fellowship, Faculty of Medicine and Human Sciences, University of Manchester.

References

1. Pangburn MK. Host recognition and target differentiation by factor H, a regulator of the alternative pathway of complement. *Immunopharmacology*. 2000; 49:149–157. [PubMed: 10904114]
2. Kim DD, Song WC. Membrane complement regulatory proteins. *Clin. Immunol*. 2006; 118:127–136. [PubMed: 16338172]
3. Clark SJ, Bishop PN, Day AJ. Complement factor H and age-related macular degeneration: The role of glycosaminoglycan recognition in disease pathology. *Biochem. Soc. Trans.* 2010; 38:1342–1438. [PubMed: 20863311]
4. Day AJ, Clark SJ, Bisho PN. Understanding the molecular basis of age-related macular degeneration and how the identification of new mechanisms may aid the development of novel therapies. *Expert Rev. Ophthalmol*. 2011; 6:123–128.
5. Perkins SJ, Goodship THJ. Molecular modelling of the C-terminal domains of factor H of human complement: a correlation between haemolytic uraemic syndrome and a predicted heparin binding site. *J. Mol. Biol.* 2002; 316:217–224. [PubMed: 11851332]
6. Ferreira VP, Herbert AP, Cortés C, McKee KA, Blaum BS, Esswein ST, Uhrín D, Barlow PN, Pangburn MK, Kavanagh D. The binding of factor H to a complex of physiological polyanions and C3b on cells is impaired in atypical haemolytic uremic syndrome. *J. Immunol*. 2009; 182:7009–7018. [PubMed: 19454698]
7. Edwards AO, Ritter R III, Abel KJ, Manning A, Panhuysen C, Farrer LA. Complement factor H polymorphism and age-related macular degeneration. *Science*. 2005; 308:421–424. [PubMed: 15761121]
8. Klein RJ, Zeiss C, Chew EY, Tsai JY, Sackler RS, Haynes C, Henning AK, SanGiovanni JP, Mane SM, Mayne ST, Bracken MB, Ferris FL, Ott J, Barnstable C, Hoh J. H polymorphism in age-related macular degeneration. *Science*. 2005; 308:385–389. [PubMed: 15761122]
9. Haines JL, Hauser MA, Schmidt S, Scott WK, Olson LM, Gallins P, Spencer KL, Kwan SY, Noureddine M, Gilbert JR, Schnetz-Boutaud N, Agarwal A, Postel EA, Pericak-Vance MA. Complement factor H variant increases the risk of age-related macular degeneration. *Science*. 2005; 308:419–421. [PubMed: 15761120]
10. Hageman GS, Anderson DH, Johnson LV, Hancox LS, Taiber AJ, Hardisty LI, Hageman JL, Stockman HA, Borchardt JD, Gehrs KM, Smith RJH, Silvestri G, Russell SR, Klaver CCW, Barbazetto I, Chang S, Yannuzzi LA, Barile GR, Merriam JC, Smith RT, Olsh AK, Bergeron J, Zernant J, Merriam JE, Gold B, Dean M, Allikmets R. A common haplotype in the complement regulatory gene factor H (*HFI/CFH*) predisposes individuals to age-related macular degeneration. *Proc. Natl. Acad. Sci. USA*. 2005; 102:7227–7232. [PubMed: 15870199]
11. Anderson DH, Radeke MJ, Gallo NB, Chapin EA, Johnson PT, Curletti CR, Hancox LS, Hu J, Ebright JN, Malek G, Hauser MA, Rickman CB, Bok D, Hageman GS, Johnson LV. The pivotal role of the complement system in aging and age-related macular degeneration: Hypothesis revisited. *Prog. Retin. Eye Res*. 2009; 29:95–112. [PubMed: 19961953]
12. Clark SJ, Perveen R, Hakobyan S, Morgan BP, Sim RB, Bishop PN, Day AJ. Impaired binding of the AMD-associated complement factor H 402H allotype to Bruch's membrane in human retina. *J. Biol. Chem*. 2010; 285:30192–30202. [PubMed: 20660596]
13. Raychaudhuri S, Iartchouk O, Chin K, Tan PI, Tai AK, Ripke S, Gowrisankar S, Vemuri S, Montgomery K, Yu Y, Reynolds R, Zack DJ, Campochiaro B, Campochiaro P, Katsanis N, Daly MJ, Seddon JM. A rare penetrant mutation in CFH confers high risk of age-related macular degeneration. *Nat. Genet*. 2011; 43:1232–1236. [PubMed: 22019782]
14. Coleman HR, Chan CC, Ferris FL, Chew EY. Age-related macular degeneration. *Lancet*. 2008; 372:1835–1845. [PubMed: 19027484]
15. Kazatchkine MD, Fearon DT, Silbert JE, Austen KF. Surface-associated heparin inhibits zymosan-induced activation of the human alternative complement pathway by augmenting the regulatory action of the control proteins on particle-bound C3b. *J. Exp. Med*. 1979; 150:1202–1215. [PubMed: 501288]
16. Meri S, Pangburn MK. Regulation of alternative pathway complement activation by glycosaminoglycans: specificity of the polyanion binding site on factor H. *Biochem. Biophys. Res. Commun*. 1994; 198:52–59. [PubMed: 8292049]

17. Ripoché J, Day AJ, Harris TJR, Sim RB. The complete amino acid sequence of human complement factor H. *Biochem. J.* 1988; 249:593–602. [PubMed: 2963625]
18. Blackmore TK, Sadlon TA, Ward HM, Lublin DM, Gordon DL. Identification of a heparin binding domain in the seventh short consensus repeat of complement factor H. *J. Immunol.* 1996; 157:5422–5427. [PubMed: 8955190]
19. Blackmore TK, Hellwage J, Sadlon TA, Higgs N, Zipfel PF, Ward HM, Gordon DL. Identification of the second heparin-binding domain in human complement factor H. *J. Immunol.* 1998; 160:3342–3348. [PubMed: 9531293]
20. Clark SJ, Higman VA, Mulloy B, Perkins SJ, Lea SM, Sim RB, Day AJ. H384 allotypic variant of factor H associated with age-related macular degeneration has different heparin-binding properties from the non-disease-associated form. *J. Biol. Chem.* 2006; 281:24713–24720. [PubMed: 16787919]
21. Herbert AP, Uhrín D, Lyon M, Pangburn MK, Barlow PN. Disease-associated sequence variations congregate in a polyanion recognition patch on human factor H revealed in three-dimensional structure. *J. Biol. Chem.* 2006; 281:16512–16520. [PubMed: 16533809]
22. Herbert AP, Deakin JA, Schmidt CQ, Blaum BS, Egan C, Ferreira VP, Pangburn MK, Lyon M, Uhrín D, Barlow P. Structure shows that a glycosaminoglycan and protein recognition site in factor H is perturbed by age-related macular degeneration-linked single nucleotide polymorphism. *J. Biol. Chem.* 2007; 282:18960–18968. [PubMed: 17360715]
23. Prosser BE, Johnson S, Roversi P, Herbert AP, Blaum BS, Tyrrell J, Jowitt TA, Clark SJ, Tarelli E, Uhrín D, Barlow PN, Sim RB, Day AJ, Lea SM. Structural basis for complement factor H-linked age-related macular degeneration. *J. Exp. Med.* 2007; 204:2277–2283. [PubMed: 17893204]
24. Schmidt CQ, Herbert AP, Kavanagh D, Gandy C, Fenton CJ, Blaum BS, Lyon M, Uhrín D, Barlow PN. A new map of glycosaminoglycan and C3b binding sites on factor H. *J. Immunol.* 2008; 181:2610–2619. [PubMed: 18684951]
25. Herbert AP, Kavanagh D, Johansson C, Morgan HP, Blaum BS, Hannan JP, Barlow PN, Uhrín D. Structural and functional characterization of the product of disease-related factor H gene conversion. *Biochemistry.* 2012; 51:1874–1884. [PubMed: 22320225]
26. Day AJ, Willis AC, Ripoché J, Sim RB. Sequence polymorphism of human complement factor H. *Immunogenetics.* 1988; 27:211–214. [PubMed: 2962936]
27. Hecker LA, Edwards AO, Ryu E, Tosakulwong N, Baratz KH, Brown WL, Issa PC, Scholl HP, Pollok-Kopp B, Schmid-Kubista KE, Bailey KR, Oppermann M. Genetic control of the alternative pathway of complement in humans and age-related macular degeneration. *Hum. Mol. Genet.* 2010; 19:209–215. [PubMed: 19825847]
28. Józsi M, Oppermann M, Lambris JD, Zipfel PF. The C-terminus of complement factor H is essential for host cell protection. *Mol. Immunol.* 2007; 44:2697–2706. [PubMed: 17208302]
29. Hakobyan S, Harris CL, van den Berg CW, Fernandez-Alonso MC, de Jorge EG, Rodriguez de Cordoba S, Rivas G, Mangione P, Pepys MB, Morgan BP. Complement factor H binds to denatured rather than to native pentameric C-reactive protein. *J. Biol. Chem.* 2008; 283:30451–30460. [PubMed: 18786923]
30. Mulloy B, Gray E, Barrowcliffe TW. Characterization of unfractionated heparin: comparison of materials from the last 50 years. *Thromb. Haemost.* 2000; 84:1052–1056. [PubMed: 11154113]
31. Mahoney DJ, Blundell CD, Day AJ. Mapping the hyaluronan-binding site on the link module from human tumor necrosis factor-stimulated gene-6 by site-directed mutagenesis. *J. Biol. Chem.* 2001; 276:22764–22771. [PubMed: 11287417]
32. Mulloy B, Forster MJ, Jones C, Drake AF, Johnson EA, Davies DB. The effect of variation of substitution on the solution conformation of heparin: a spectroscopic and molecular modeling study. *Carbohydr. Res.* 1994; 255:1–26. [PubMed: 8181000]
33. Ostrovsky O, Berman B, Gallagher J, Mulloy B, Fernig DG, Delehedde M, Ron D. Differential effects of heparin saccharides on the formation of specific fibroblast growth factor (FGF) and FGF receptor complexes. *J. Biol. Chem.* 2002; 277:2444–2453. [PubMed: 11714710]
34. Marson A, Robinson DE, Brookes PN, Mulloy B, Wiles M, Clark SJ, Fielder HL, Collinson LJ, Cain SA, Kieley CM, McArthur S, Buttle DJ, Short RD, Whittle JD, Day AJ. Development of a

- microtiter plate-based glycosaminoglycan array for the investigation of glycosaminoglycan-protein interactions. *Glycobiology*. 2009; 19:1537–1546. [PubMed: 19729381]
35. Sim E, Palmer MS, Puklavec M, Sim RB. Monoclonal antibodies against the complement control protein factor H (beta 1 H). *Biosci. Rep.* 1983; 3:1119–1131. [PubMed: 6199050]
 36. Lohse DL, Linhardt RJ. Purification and characterization of heparin lyases from *Flavobacterium heparinum*. *J. Biol. Chem.* 1992; 267:24347–24355. [PubMed: 1332952]
 37. Gu K, Linhardt RJ, Laliberté M, Gu K, Zimmermann J. Purification, characterization and specificity of chondroitin lyases and glycuronidase from *Flavobacterium heparinum*. *Biochem. J.* 1995; 312:569–577. [PubMed: 8526872]
 38. Esko J, Selleck SB. Order out of chaos: Assembly of ligand binding sites in heparan sulfate. *Annu. Rev. Biochem.* 2002; 71:435–471. [PubMed: 12045103]
 39. Khan S, Nan R, Gor J, Mulloy B, Perkins SJ. Bivalent and co-operative binding of complement factor H to heparan sulfate and heparin. *Biochem. J.* 2012; 444:417–428. [PubMed: 22471560]
 40. Clark SJ, Keenan TDL, Fielder HL, Collinson LJ, Holley RJ, Merry CLR, van Kuppevelt TH, Day AJ, Bishop PN. Mapping the differential distribution of glycosaminoglycans in the adult human retina, choroid, and sclera. *Invest. Ophthalmol. Vis. Sci.* 2011; 52:6511–6521. [PubMed: 21746802]
 41. Wright AF. A rare variant in CFH directly links age-related macular degeneration with rare glomerular nephropathies. *Nat. Genet.* 2011; 43:1176–1177. [PubMed: 22120053]
 42. Manuelian T, Hellwage J, Meri S, Caprioli J, Noris M, Heinen S, Józsi M, Neumann HPH, Remuzzi G, Zipfel PF. Mutations in factor H reduce binding affinity to C3b and heparin and surface attachment to endothelial cells in haemolytic uremic syndrome. *J. Clin. Invest.* 2003; 111:1181–1190. [PubMed: 12697737]
 43. Józsi M, Heinen S, Hartmann A, Ostrowicz CW, Hälbig S, Richter H, Kunert A, Licht C, Saunders RE, Perkins SJ, Zipfel PF, Skerka C. Factor H and atypical haemolytic uremic syndrome: Mutations in the C-terminus cause structural changes and defective recognition functions. *J. Am. Soc. Nephrol.* 2006; 17:170–177. [PubMed: 16338962]
 44. Sánchez-Corral P, Pérez-Caballero D, Huarte O, Simckes AM, Goicoechea E, López-Trascasa M, Rodríguez de Córdoba S. Structural and functional characterization of factor H mutations associated with atypical haemolytic uremic syndrome. *Am. J. Hum. Genet.* 2002; 71:1285–1295. [PubMed: 12424708]
 45. Booi JC, Baas DC, Beisekeeva J, Gorgels TGMF, Bergen AAB. The dynamic nature of Bruch's membrane. *Prog. Retin. Eye Res.* 2010; 29:1–18. [PubMed: 19747980]
 46. Weismann D, Hartvigsen K, Lauer N, Bennett KL, Scholl HPN, Issa PC, Cano M, Brandstatter H, Tsimikas S, Skerka C, Superti-Furga G, Handa JT, Zipfel PF, Witztum JL, Binder CJ. Complement factor H binds malondialdehyde epitopes and protects from oxidative stress. *Nature.* 2011; 478:76–81. [PubMed: 21979047]
 47. Sjöberg AP, Trouw LA, Clark SJ, Sjölander J, Heinegård D, Sim RB, Day AJ, Blom AM. The factor H variant associated with age-related macular degeneration (His-384) and the non-disease-associated form bind differentially to C-reactive protein, fibromodulin, DNA, and necrotic cells. *J. Biol. Chem.* 2007; 282:10894–10900. [PubMed: 17293598]
 48. Laine M, Jarva H, Seitonen S, Haapasalo K, Lehtinen MJ, Lindeman N, Anderson DH, Johnson PT, Järvelä I, Jokiranta TS, Hageman GS, Immonen I, Meri S. Y402H polymorphism of complement factor H affects binding affinity to C-reactive protein. *J. Immunol.* 2007; 178:3831–3836. [PubMed: 17339482]
 49. Lauer N, Mihlan M, Hartmann A, Schlötzer-Schrehardt U, Keilhauer C, Scholl HPN, Issa PC, Holz F, Weber BHF, Skerka C, Zipfel PF. Complement regulation at necrotic cell lesions is impaired by the age-related macular degeneration-associated factor H His402 risk variant. *J. Immunol.* 2011; 187:4374–4383. [PubMed: 21930971]
 50. Smith RJH, Alexander J, Barlow PN, Botto M, Cassavant TL, Cook HT, Rodríguez de Córdoba S, Hageman GS, Jokiranta TS, Kimberling WJ, Lambris JD, Lanning LD, Levidiotis V, Licht C, Lutz HU, Meri S, Pickering MC, Quigg RJ, Rops AL, Salant DJ, Sethi S, Thurman JM, Tully HF, Tully SP, van der Vlag J, Walker PD, Würzner R, Zipfel PF. New approaches to the treatment of dense deposit disease. *J. Am. Soc. Nephrol.* 2007; 18:2447–2456. [PubMed: 17675665]

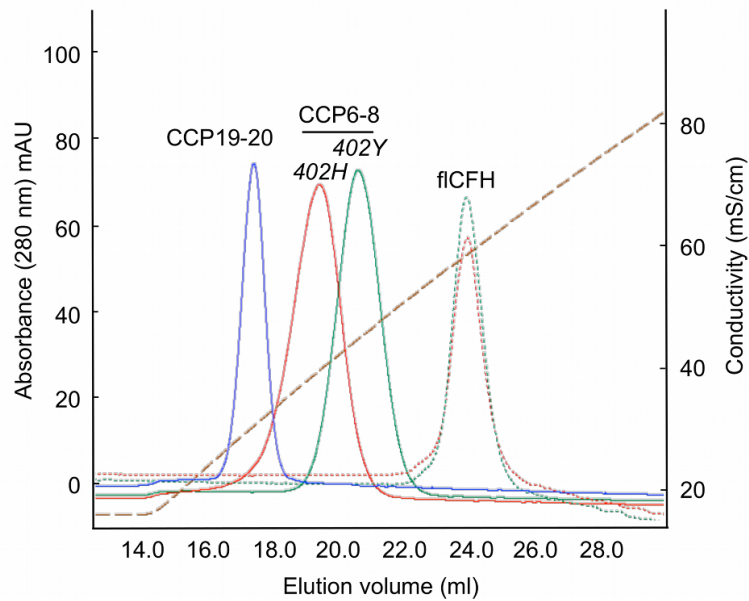


Figure 1. CCP19-20 binds poorly to heparin compared to CCP6-8

Recombinant CCP19-20 (blue), and the 402H (red) and 402Y (green) variants of CCP6-8 (solid lines) and fICFH (dotted lines) were analyzed using heparin affinity chromatography. The proteins were eluted using a NaCl gradient (conductivity denoted by brown dashed line) where the absorbance was monitored at 280 nm; these data are representative of at least two independent experiments. The differential (salt-dependent) binding strength of the 402H and 402Y CCP6-8 variants is consistent with our previous results on a HiTrap Heparin column (12, 20). The lack of differential binding between the 402H and 402Y forms of fICFH is likely to be due to the highly sulfated nature of the heparin used here and the consequent lack of resolution of the column when two binding sites (CCP6-8 and CCP19-20) are both contributing to the avidity.

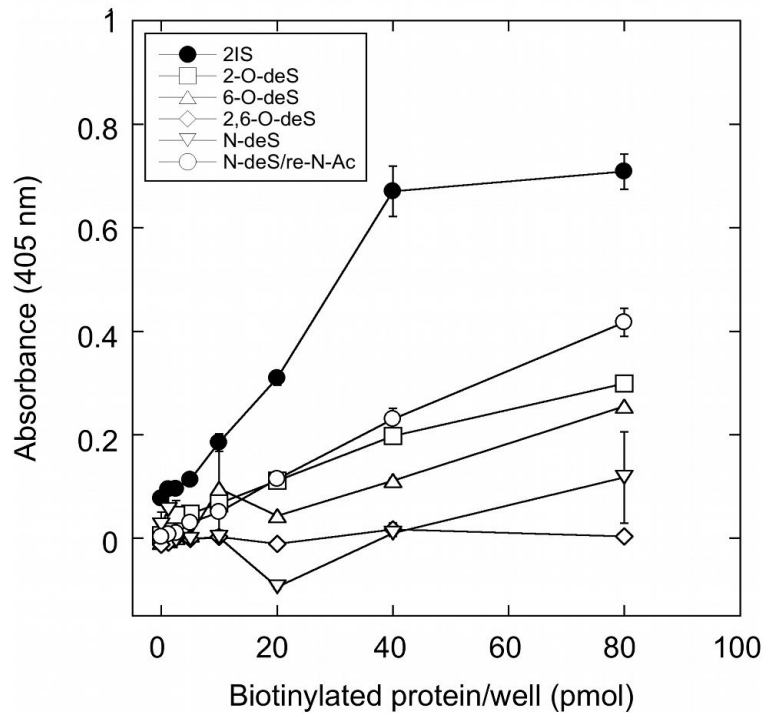


Figure 2. Sulfate groups of heparin play a major role in CCP19-20 binding

The interaction of biotinylated CCP19-20 with immobilized heparin preparations was determined using the microtiter plate assay described before (20); heparin was either untreated (2IS: ●) or had been selectively desulfated: 2-O-desulfated (□); 6-O-desulfated (△); 2,6-O-desulfated (◇); N-desulfated (▽); N-desulfated re-N-acetylated (○). All values are plotted as mean absorbance (at 405 nm) determined from two independent experiments ($n=4$) \pm s.e.m. The CCP6-8 402H and 402Y variants were used as controls in these experiments (Supplemental Fig.3) and gave essentially identical results to those published previously (20,23).

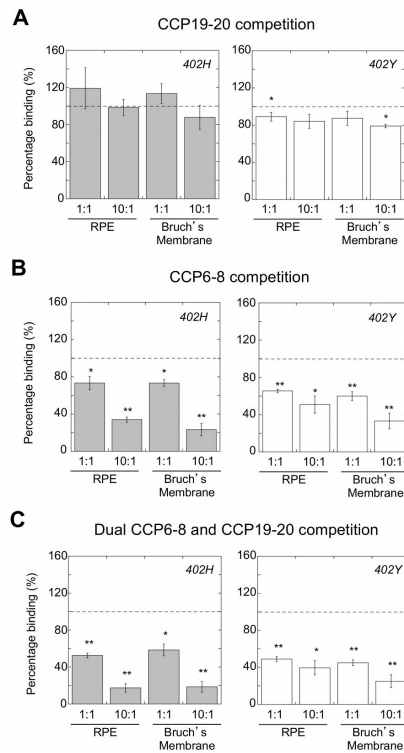


Figure 3. CCP6-8 contributes more than CCP19-20 to fICFH binding in macula tissue
 The 402H and 402Y forms of fICFH (fluorescently labeled with AlexaFluor594 and AlexaFluor488, respectively) were incubated with human tissue sections in the absence or in the presence of 1- or 10-fold molar excess CCP19-20 (A) or CCP6-8 (B) or CCP6-8 and CCP19-20 together (C); in (B) and (C) matching allotypes of CCP6-8 and fICFH were used (i.e. either 402H vs 402H or 402Y vs 402Y). In each case, the relative fluorescence was measured for the RPE and Bruch's membrane from five different donors after subtracting autofluorescence from blanks, and the data are plotted as percentage binding for fICFH in the absence of competitor \pm s.e.m. Data were analyzed (compared to non-competed) using a paired Student's t test where $P < 0.05$ was considered to represent a significant difference; * = $P < 0.05$ and ** = $P < 0.001$.

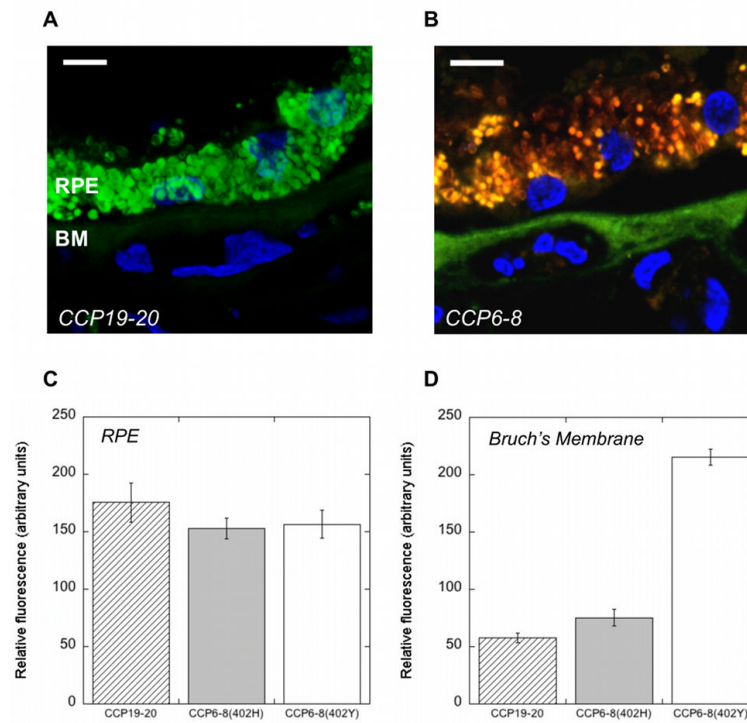


Figure 4. Comparison of CCP19-20 and CCP6-8 binding sites in the RPE and Bruch's membrane of human macula tissue

(A) CCP19-20 (green) and (B) CCP6-8 (402H (red) and 402Y (green)) were exogenously applied to human macula tissue in order to detect their binding sites within RPE and Bruch's membrane (BM). In (B) the 402H and 402Y forms of CCP6-8 were added simultaneously giving rise to yellow/orange staining at sites where they bind equivalently. The relative fluorescence values measured for each protein was averaged over all 5 donors (as listed in Table 1) where the autofluorescence from blanks had been subtracted for each donor. Data are compared for the RPE (C) and Bruch's membrane (D) and are shown as mean value \pm s.e.m. Images in (A) and (B) are from donor M12109 (Table 1) and are representative of the 5 individual donors analyzed; cell nuclei are stained with DAPI (blue) and scale bars correspond to 10 μ m.

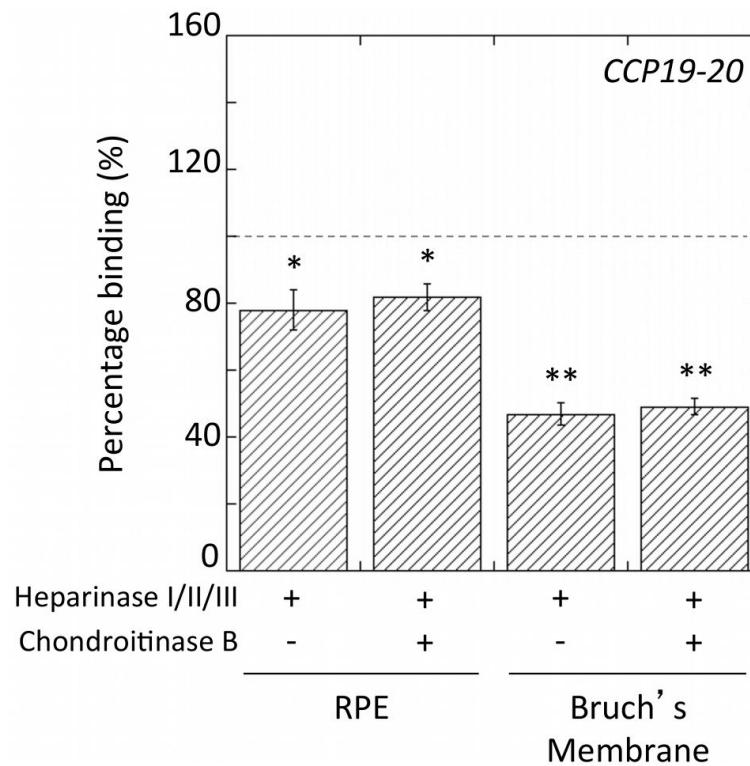


Fig. 5. Role of GAGs in the binding of CCP19-20 to human macula

The binding of fluorescently labeled CCP19-20 to RPE and Bruch's membrane was measured following enzymatic pre-treatments with a mixture of heparinase I, II, III in the absence or presence of chondroitinase B, i.e. to remove either HS alone or DS/HS together. Data from 5 donor eyes (see Table 1) were averaged and plotted as the percentage of binding seen for CCP19-20 in the absence of enzyme pre-treatment \pm s.e.m. Data were analyzed using a paired Student's t test where $P < 0.05$ was considered to represent a significant difference; * = $P < 0.05$ and ** = $P < 0.001$.

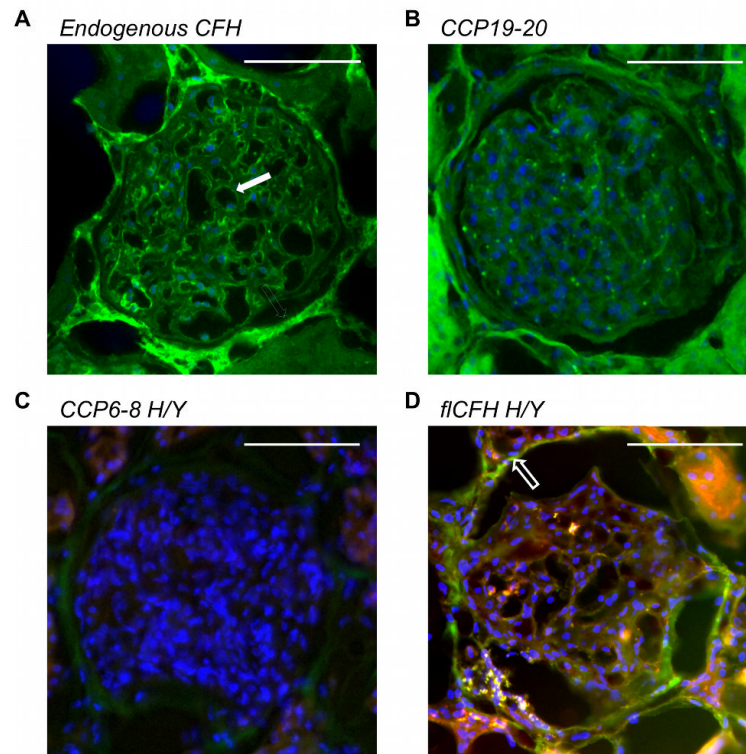


Figure 6. Localization of endogenous CFH and CFH-, CCP6-8- and CCP19-20-binding sites in human kidney

(A) Endogenously expressed CFH was detected in the glomeruli of human kidney using the OX23 antibody (green); particularly intense staining was seen within the Bowman's capsule (solid arrows) and, to a lesser extent, for the GBM (open arrows). (B) CCP19-20-binding sites were detected with fluorescently labeled CCP19-20 (green). (C) CCP6-8-binding sites were stained for with fluorescently labeled 402H (red) and 402Y (green) variants of CPP6-8. (D) CFH-binding sites were visualized using fluorescently labeled 402H (red) and 402Y (green) variants of fICFH that were exogenously applied to the kidney tissue (the Bowman's capsule is indicated by a solid arrow). All images are from donor NHK9 (Table 1) and are representative of the three separate kidney donors analyzed; cell nuclei are stained with DAPI (blue) and scale bars correspond to 100 μ m.

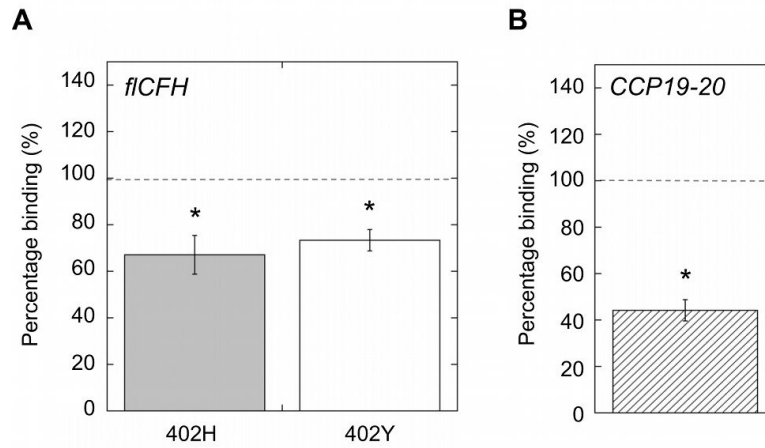


Figure 7. Role of GAGs in the binding of CFH to glomeruli

The binding of fluorescently labelled 402H and 402Y variants of fICFH (A) or fluorescently labelled CCP19-20 (B) to sites within the glomeruli of human kidneys was determined with and without enzymatic pre-treatments (a mixture of heparinase I, II, III and chondroitinase B), i.e. to remove both HS and DS. Data for 10 entire glomeruli from each of three donors (see Table 1) were averaged and plotted as the percentage of binding seen for the respective CFH proteins in the absence of enzyme pre-treatment \pm s.e.m. Data were analyzed using a paired Student's t test where $P < 0.05$ (*) was considered to represent a significant difference.

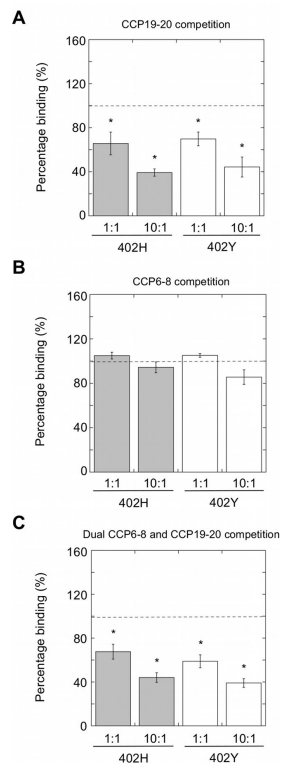


Figure 8. CP19-20 contributes more to the binding of fICFH to human kidney glomeruli than CCP6-8

The 402H (grey bars) and 402Y (white bars) variants of fICFH were incubated with human kidney tissue sections in the absence or presence of 1- or 10-fold molar excess CCP19-20 (A), CCP6-8 (B) or CCP6-8 and CCP19-20 together (C); in (B) matching allotypes of CCP6-8 and fICFH were used (i.e. either 402H vs 402H or 402Y vs 402Y). In each case the relative fluorescence of the whole glomeruli (designated here as tissue within the Bowman's space) was measured and the data plotted as a percentage binding compared to non-competed fICFH: mean data are plotted for each of three donor samples (each averaged from 10 glomeruli) \pm s.e.m. Statistical analysis was performed using a paired Student's t test, where $P < 0.05$ was considered to be significant; * = $P < 0.05$.

Table 1

Details of the donor tissue used in binding experiments.

Human eye tissue *			
<i>Donor no.</i>	<i>Sex</i>	<i>Age</i>	<i>Days Post Mortem †</i>
M12103	F	82	1
M12107	M	81	1
M12109	F	70	1
M12189	M	64	2
M12190	M	58	2
Human kidney tissue ‡			
RW1	F	54	N/A §
NHK6	M	37	N/A §
NHK9	M	49	N/A §

* All human eye samples used in this study are from genotyped individuals who were CFH 402 H/Y heterozygotes and who did not have AMD.

† The number of days macula were collected and fixed after death.

‡ Human kidney tissue was from donors without aHUS or other kidney disease.

§ These samples were excised from unused donor kidneys perfused with transplant solution and that had been kept on ice.